ZJE - 176 1976

L. Pečínka

THE PROPAGATION OF PRESSURE PULSATIONS IN THE PRIMARY CIRCUIT OF POWER PLANT A 1

ŠKODA WORKS
Nuclear Power Construction Department, Information Centre
PLZEŇ - CZECHOSLOVAKIA

ZJE - 176 1976

L. Pečínka

THE PROPAGATION OF PRESSURE PULSATIONS IN THE PRIMARY CIRCUIT OF POWER PLANT A 1

Reg. č. ÚVTEI 73307

ŠKODA WORKS
Nuclear Power Construction Department, Information Centre
PLZEŇ, CZECHOSLOVAKIA

Abstract

The forced circulation of reactor coolant (either liquid or gas) represents a source of exciting forces which in several cases caused serious faults of important reactor core components, which in turn resulted in long reactor outages and large economic losses. According to the experience, even in the feed water systems of current conventional power plants are being found faults of similar character.

It is the aim of this article to generalize the experience, gained during the time of construction of power plant A 1 for any closed piping system in which forced circulation takes place.

Classification of the exciting forces

The forced circulation of reactor coolant (or feed water) represents a source of exciting forces of hydrodynamic and acoustic type or Karman's vortex street, which in interaction with reactor core or primary circuit components causes mechanical vibrations.

The hydrodynamic exciting forces are turbulent pressure pulsations within boundary layer. The acoustic exciting forces can be fully derived from the basic laws of mechanics concerning acoustics. The following classification is applied :

- hydraulic pressure pulsations (HPP), generated by circulators (for further information see /1/)
- acoustic pressure pulsations (APP), described by the wave equation
- standing waves of organ-type, typical in primary circuits of LWR's (similar to the effects in feeding water systems of conventional power plants). The frequency spectrum is described as

$$f_1 = 0.25 \frac{c_1}{L} \quad ; \quad f_m = (2m-1) f_1 \qquad m \geq 2$$

for a tube with one end open, and

$$f_1 = 0.5 \frac{c_1}{L} \quad ; \quad f_m = m f_1 \qquad m \geq 2$$

for a pipe with both ends open.

So far we reviewed all forces having discrete frequency spectrum.

Forces with continuous frequency spectrum are as follows :

- the noise emitted by circulators (for further information see /1/),

- the pseudonoise (turbulent noise) generated by the sheer stresses in the core of turbulent stream and mainly in turbulent boundary layer.

The Karman´s vortex street arises when cross-flow is involved. This takes place in the case of valves or thermometric detectors. As stated e.g. in /8/ numerous failures occurred. Theoretical knowledge of interest is summarized in /19/. Effects of this type are not investigated here.

In the following, several remarks on the question of exciting forces in fluids and gases are given. Theoretical considerations lead to the conclusion that exciting forces energy is decreased by

- thermoviscous absorption
- energy exchange between the fluid and the pipe wall (for more details see /2/).

So the damping depends on thermodynamic parameters of fluid and on the shape of piping system.

Experiments had been performed to determine damping characteristic of gases.
Results are presented in fig. 1 and fig. 2 for CO_2 and N_2, showing that the thermoviscous absorption may be neglected. For liquids no experiments had been done.

The propagation of pressure pulsations in piping systems

Assuming that

$$\frac{p - p_0}{p_0} \ll 1$$

and that

- the thermoviscous absorption is negligible,
- the correlation between noise and discrete term is negligible

/

- the dispersion of hydraulic pressure pulsations or acoustic pressure pulsations on the noise component is negligible,

then the propagation of HPP or APP can be described by wave equation

$$\nabla^2 \phi = \frac{1}{C_0^2} \frac{\partial^2 \phi}{\partial t^2} \qquad (1)$$

which after Fourier's transformation takes the form of

$$\nabla^2 \hat{\phi} + k_0^2 \hat{\phi} = 0 \qquad k_0^2 = \frac{\omega^2}{C_0^2} \qquad (2)$$

The general solution of (2) is

$$\hat{\phi}_{n,m}(r,\theta,z,\omega) = \sum_{n=0}^{+\infty} \sum_{m=1}^{+\infty} J_m(\varkappa_{n,m} r)\left[A_{n,m} e^{-i\beta_{n,m} z} + B_{n,m} e^{i\beta_{n,m} z}\right] * \left[C_{n,m} e^{-in\theta} + D_{n,m} e^{in\theta}\right] \qquad (3a)$$

$$\frac{\omega^2}{C_0^2} = \varkappa_{n,m}^2 + \beta_{n,m}^2 \qquad (3b)$$

where the term $J_m(\varkappa_{n,m} r)$ describes the HPP field in radial, $\exp[\pm i\beta_{n,m} z]$ in axial and $\exp[\pm in\theta]$ in circumferential direction. Using (3a), the following terms may be determined;

- fluid velocity

$$\vec{U} = -\nabla\phi = U_r \vec{r} + U_\theta \vec{\theta} + U_z \vec{z} \qquad (4)$$

- acoustic pressure

$$P(r,\theta,z,t) = \rho \frac{\partial \phi}{\partial t} \qquad (5)$$

The ways in which the HPP and APP proceed in axial direction can be investigated using the equation (3b). The following three cases are possible :

- $\beta^2_{n,m} = \frac{\omega^2}{c_0^2} - \varkappa^2_{n,m} > 0$ propagation in z-direction,
- $\beta^2_{n,m} = \frac{\omega^2}{c_0^2} - \varkappa^2_{n,m} < 0$ exponential damping in z - direction
- $\beta^2_{n,m} = \frac{\omega^2}{c_0^2} - \varkappa^2_{n,m} = 0$ limiting case, propagation not dependent on the z - coordinate

The frequecies corresponding to the limit-ing case are called characteristic frequencies $f^c_{n,m}$ (modal cut-off) and for the case of rigid infinite duct are determined from the condition of zero velocity in radial direction at $r = r_0$, which in turn leads to

$$\frac{\partial}{\partial r}\left[J_n(\varkappa_{n,m} r)\right]_{r=r_0} = 0 \qquad (6)$$

Hence $f^c_{n,m} = \varkappa_{n,m} c_0 / d_0$, the values of $\varkappa_{n,m}$ for $n \in \langle 0, 4 \rangle$ $m \in \langle 1, 5 \rangle$ are in tab. 1.

From the form of the term $\left[C_{n,m} e^{-in\theta} - D_{n,m} e^{+in\theta}\right]$ in (3a) is clear that the wave propagation takes place in circumferential direction, too.

From (3a) it is clear that the values of m refer to radial pressure distribution and determine the number of so called nodal curves.

Examples

n = 0, m = 1

The basic case, plene wave which at certain conditions propagates in z-direction within the whole frequency spectrum with the velocity of sound in given medium. Wave length $\lambda_{0,1} = \frac{c_0}{f_{0,1}}$, see fig. 3.

$n = 0, m = 2$

Pressure distribution in radial direction takes place, the characteristic frequency being $f_{0,2} = 1.2197\, c_0 d_0^{-1}$. Pressure disturbations in axial direction travel with velocity $U_{0,2}$ which is smaller than corresponding sound velocity. Wave length $\lambda_{0,2} = 2\pi \beta_{0,2}^{-1}$ is determined on the basis of axial wave number $\beta_{0,2}$ from eq. (3b) and is always different from $c_0 f_{0,2}^{-1}$ whose use lacks in this case physical justification. Pressure distribution throughout the cross-section is given in fig. 4.

n = 1, m = 2

General case, pressure changes in radial and circumferential direction. Number of nodal points 2 n = 2, $f_{1,2} = 2.1346\, c_0 d_0^{-1}$. Pressure disturbations in axial direction travel with the velocity $U_{1,2}$, which is smaller than sound velocity in given environment. The wave length is determined as in the preceding case from $\lambda_{1,2} = 2\pi \beta_{1,2}^{-1}$. Pressure distribution is shown in fig. 5.

It appears that, for practical purposes, systems can be reduced to the scheme: disturbation source → waveguide → volume (e.g.gas tank, instrument chamber).

From theoretical considerations follows that for identification of pressure pulsations propagating in a piping system, the knowledge of frequency and pressure distribution in a plane perpendicular to z-direction is required (which is equivalent to the knowledge of a pair of modal numbers $[n, m]$. The wave length is to be determined very carefully, taking into account that for all $n > 0, m \geq 1$ and $n = 0, m > 1$ holds the relation $f \geq f_{n,m}$.

The method of measuring discrete frequency components

Based on the introducing assumption of preceding paragraph the problems of measurements may be formulated as the problem of selecting a periodical signal from random noise. Two methods of approach to this problem exist : deterministic and stochastic. Both methods make use of harmonical analysis, based either on convenient computer algorithm or standard frequency analyzer with minimum bandwidth of 1/3 octave.

The results of deterministic method are expressed in the form of a frequency to amplitude function. The results of many measurements show that the dispersion of results (for a given frequency and sufficiently long time period) represents about 10 dB, which is rather significant error. Theoretical discussion of this fact based on the analysis of eq. (3a) had shown that (according to /7/) the main reasons for this are :

- instabilities of fluid thermodynamic parameters
- possible changes of modal number pairs during the wave propagation
- changes in the speed of circulator.

The disadvantages just described are eliminated by the statistical approach, assuming that the process of discrete components propagation bears the character of a steady - state ergodic random process. The amplitude values of given frequencies are interpreted as a continuous random function which may be described either by first type characteristic (the distribution function and mean values), or by second type characteristic represented by correlation functions or power spectral densities (auto- and cross correlation). Most frequently the spectral densities are used. The mathematical model is rather complicated, and is partly solved in /4/ to /7/.

The statistical treatment of signals is - according to the current state of computer technology - performed by :

- analog method
- analog-digital method
- special hybride-system method

The analog methods work according to the scheme : measuring recorder → standard correlation equipment or frequency analyzer with some convenient filter.
The disadvantage of this method is a long evaluation time and low accuracy. The analog-digital methods are based on the following scheme : a fast analog-digital transformer (if possible with auxiliary memory) → digital computer with high speed printing unit and, if possible, a parallel - connected spectrum analyzer. This arrangement has several advantages :

- considerable acceleration of evaluatin process
- the prompt spectrum analyzer enables visual control of the process and enables to decide, which time interval is of interest for detail investigation.

The computation of values defined by (2) - (4) is made by computer.

The hybrid systems perform at least the 1/3 octave or narrow band frequency analysis in real time and, using routine programs, calculate and print the results of eq. (2) - (4) and other, if needed. With regard to the fact that equipment used is of rather small size, on-line evaluation is possible.

The generalization of measurement results

It was shown that dimensionless parameters describing propagation of HPP in a piping system may be formed as follows :

Sh number = $f D_0 \left(\frac{\Delta p}{\rho}\right)^{-\frac{1}{2}}$, it is the HPP source characteristic

*Ma, Re number, it is the fluid thermodynamic characteristic.

Sh number = $f l c_0^{-1}$, it is the APP or tube characteristic.

The dimensionless HPP amplitude may be chosen in the following manner :

- in the case of a deterministic approach

$$\frac{P(r, \theta, z)}{\rho c_0^2}$$

- in the case of a statistical approach either

$$\frac{S_p(\omega)}{\rho^2 c_0^4}\,\frac{1}{l} \quad or \quad \frac{\langle \overline{P^2(r, \theta, z)} \rangle}{\rho^2 c_0^4}$$

The dimensionless parameters are of great importance when the actual equipment parameters are to be determined on the basis of model measurements.

<u>The HPP measurements on the A 1 power plant</u>

Some procedures, described in previous parts, had been applied when measurements of HPP in selected parts of nuclear power plant A 1 were done. The aim of these measurements, performed during the preoperational period of A 1 start-up, was to investigate the influence of primary circuit geometry on the HPP level which in turn had to make possible the usage of research results gained at the test facility for operational conditions of power plant primary circuit.

The experiments were performed in the piping of circulator No 3. The schematic illustration of loop arrangement is in fig. 6.

During the HPP measurements the reactor was filled with dummy fuel elements, the two remaining circulators No 1 and No 2 being in operation, too.

Because the preoperational test schedule did not consider placing of measuring equipment, the sensors, when installed, were not in the proper position parallel to the inner surface of the main piping, which in turn gave rise to many troubles during preparing and evaluating the measurement.
The equippment localisation was, according to existing situation, designed with the aim of minimum distortion of HPP main frequency components, which corresponds to minimum number of peaks of transfer function in a given frequency interval. The form of sensor bungs was based on theoretical analysis and their final shape was tested for the correction of transfer characteristics. Measurements of Y functions were made in an acoustic box. The results for the point E1 (see fig. 6) can be seen in fig. 7a and 7b.

This example shows the change of transfer function, too. As testing was made with air at atmospheric pressure, then, provided that calculated and measured values of $|Y| = f(\omega)$ are equal, the same mathematical model may be used for calculation of $|Y|$ for ρ and c_0 values, corresponding to A 1 coolant parameters during the tests.

As HPP sensor a piezoelectric unit developed by Škoda - ZVJE was used (fig. 7). The records of signals were made using Bell-Howell equipment. During measurement analysis, Brüel & Kjaer analyzer and recorder were used and, after the transformation to digital form, the computer NE 803 was used to perform the Fourier's analysis.

During the measurements, the effect of circulator TK3 mass flow ratio was investigated as well as that of TK3 control blades position on the HPP level. The coolant parameters during the investigation period were roughly constant, p_s = 5.3 MPa. Failures of several sensors took place and some pluging of pressure ducts occurred. For final evaluation about 30 representative samples of records from points F1, D1, M1 and D were at disposal (fig. 6). The illustration of point D record at $G/G_{nom} = 1$, $p_s = 5.3$ MPa, $\vartheta_s = 97°C$, $\delta = 0°$ is in fig. 9. Fig. 10 shows the simplified form of $a_{p/\varphi} = f(G/G_{nom})$. All measurements may be divided in two groups : circulator inlet and circulator outlet, and for illustration the curve obtained by the circulator test (at outlet) is plotted, too. In fig. 11 the functional dependence $a_{p/\varphi} = f(\delta)$ is seen (both for primary circuit, and for circulator test); both are valid for circulator outlet.

The points, corresponding to plant measurements show values about 30% lower than those obtained with circulator. This can be caused by the following factors :

a/ inaccuracy of values of transfer functions, and higher HPP damping in the bungs

b/ the geometry of A 1 primary circuit, and the influence of HPP generated by remaining circulators

c/ pulsations damping in the primary circuit and their dissipation in reactor

d/ differences in measurement point location in primary circuit and during circulator tests

e/ the HPP time changes, i.e. the changes of frequency component amplitudes, and their mutual phase.

The last effect was investigated by means of Fourier's analysis of signals from sensor D. Based on a 180th-order Fourier polynomial with basis frequency 50 HZ, 0.1 s signal components were determined, including corresponding phase angles. The results are plotted in fig. 12 and fig. 13. Here the normalized frequency components of 50, 800, 1600 and 2400 Hz as a function of time are seen (with 400 Hz being the reference value for normalization), along with differences between phase angles of said frequencies and the reference one 400 Hz.

The main normalized frequency components of HPP amplitudes are in agreement with measurements during circulator tests. The difference is smaller than in the case of HPP amplitude level (20 - 25%). The character of the dependence of HPP level on the ratio G/G_{nom} or δ is of similar character and the displacement of higher HPP components at G/G_{nom} or δ is found to be equal to that determined during circulator tests.

The fundamental effect of damping and geometry was not established. The effect of sensors placing was partially eliminated by selecting a set of representative samples and by statistical treatment of values measured in several places.

List of symbols

a_p	amplitude of HPP $[Pa]$
A, B, C, D	constants
c_0	sound velocity $[ms^{-1}]$
d_0	piping diameter $[m]$
D_0	characteristic dimension of circulator $[m]$
f	frequency $[Hz]$
G	mass flow $[kgs^{-1}]$
J_n	Bessel function of n-th order
k_0	wave number $[m^{-1}]$
l	characteristic dimension (length or diameter of piping) $[m]$
L	length of piping
m, n	modal numbers
p	pressure fluctuation, pressure $[Pa]$
Δp	circulator pressure drop $[Pa]$
P	periodical component of pressure pulsation $[Pa]$
r	radial coordinate $[m]$
t	time $[s]$
U	velocity of coolant $[ms^{-1}]$
Y	transfer function $[1]$
z	axial coordinate (length) $[m]$
$Z_0 = \rho c_0$	acoustic impedance $[kgm^{-3}s^{-1}]$
$\alpha_{n,m}$	modal constant $[1]$
$\beta_{m,n}$	axial wave number $[m^{-1}]$
δ	control blades displacement angle $[rad]$

λ	wave length $[m]$
ϱ	density $[kg\,m^{-3}]$
ϑ	temperature $[K]$
Θ	angle coordinate $[rad]$
φ	phase displacement $[rad]$
Φ	potential function $[m^2 s^{-1}]$
ω	angle frequency, Fourier's integrating variable $[rad\,s^{-1}]$
$\hat{}$	symbol of Fourier's from of function
s	suction
$\bar{\delta}$	relative damping
$\varkappa$	specific heats ratio $[-]$
$\varkappa$	radial wave number $[m^{-1}]$

References

/1/ Němec J., Svoboda Vl. - The origin of hydraulic pressure pulsatioa in a radial compressor. Energetika 1975, No 8. p.353-358 (in Czech)

/2/ Kozák J., Pečínka L. - The dynamic response of power plant A 1 components on hydraulic pressure pulsations. Energetika 1975, No 8, p. 358-362 (in Czech)

/3/ Dyer I. - Measurement of noise sources in ducts. The Journal of ASA, 1959, 30, No 9.

/4/ Beneš J. - The statistical dynamics of control circuits. SNTL, Prague, 1961.

/5/ Pečínka L. - Dynamic effects in ducts with forced circulation. Proc.of 11th acoustic conference on noise and environment, CSSR, 1973

/6/ Pečínka L. - Diagnostics of reactor primary circuit components vibration. Proc. of 3rd CSKAE panel, Zvíkovské Podhradí, 1973

/7/ Pečínka L. - Stochastic exciting forces in nuclear power plant primary circuit. Proc.of 3rd CSKAE panel on dynamic effects in power plant primary circuit of A 1, Zvíkovské Podhradí, 1973

/8/ Kopřiva Vl. - The calculation of thermometric bungs loading. Strojírenství 1963, 13, No 4

/9/ Pětrovský Vl. - The self-controlled vibrations of elastic constructions caused by Karman´s vortex street. Proc. of 3rd CSKAE panel on dynamic effects in power plant primary circuit of A 1, Zvíkovské Podhradí, 1973.

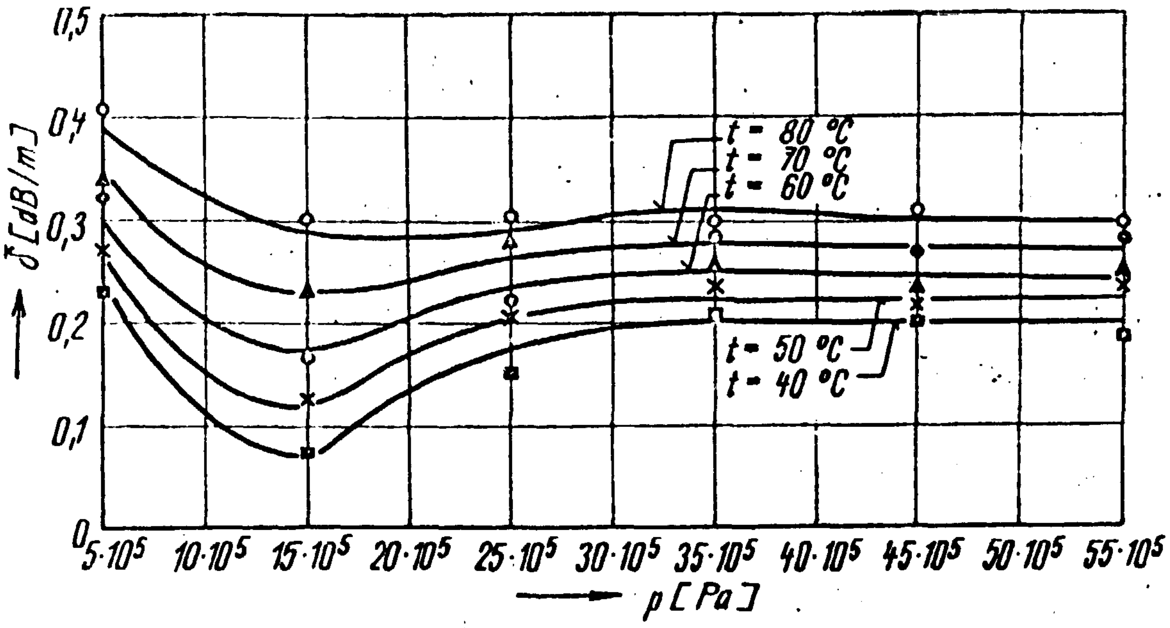
0,5
0,4
0,3
0,2
0,1
0
δ [dB/m]
t = 80 °C
t = 70 °C
t = 60 °C
t = 50 °C
t = 40 °C
5·10⁵
10·10⁵
15·10⁵
20·10⁵
25·10⁵
30·10⁵
35·10⁵
40·10⁵
45·10⁵
50·10⁵
55·10⁵
p [Pa]

Fig. 1.

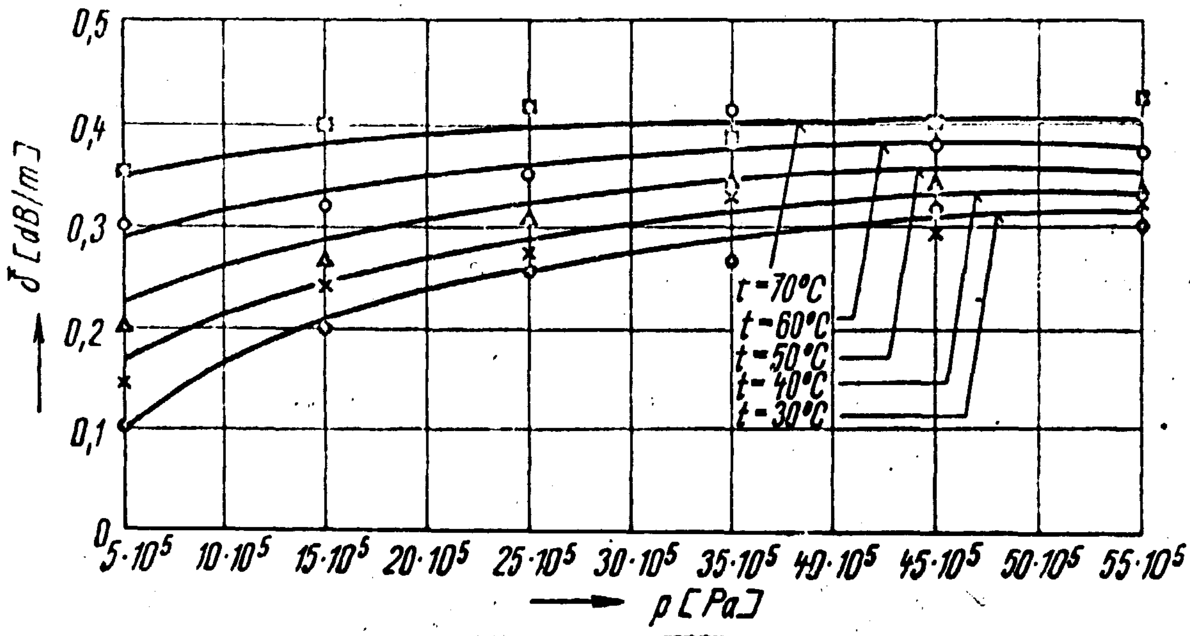
0,5
0,4
0,3
0,2
0,1
0
δ [dB/m]
t = 70°C
t = 60°C
t = 50°C
t = 40°C
t = 30°C
5·10⁵
10·10⁵
15·10⁵
20·10⁵
25·10⁵
30·10⁵
35·10⁵
40·10⁵
45·10⁵
50·10⁵
55·10⁵
p [Pa]

Fig. 2.

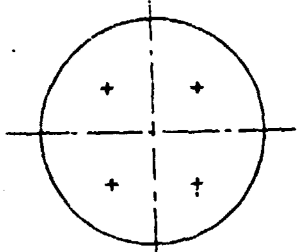

Fig. 3.

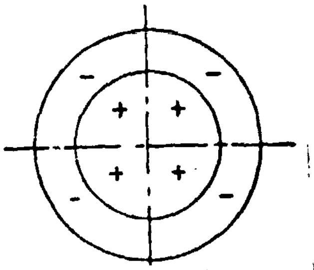

Fig. 4.

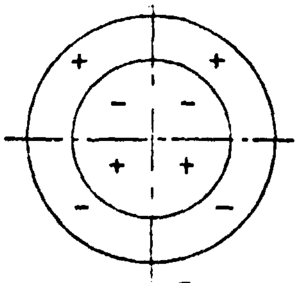

Fig 5

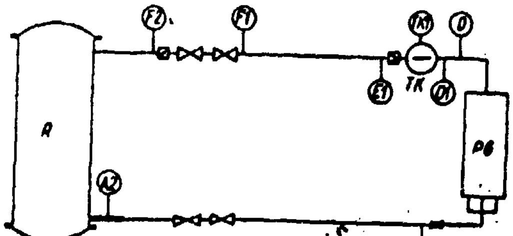

Fig. 6.

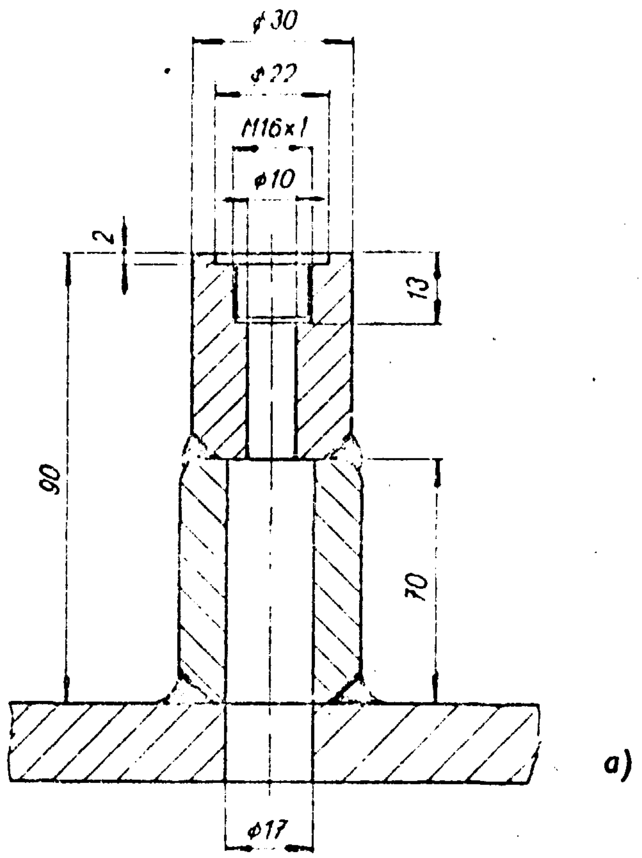

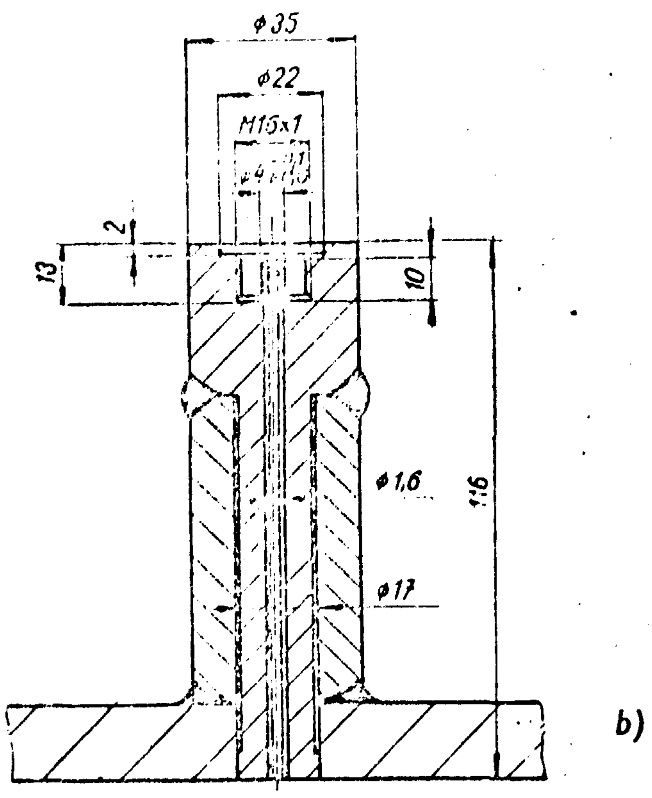

Fig. 7.

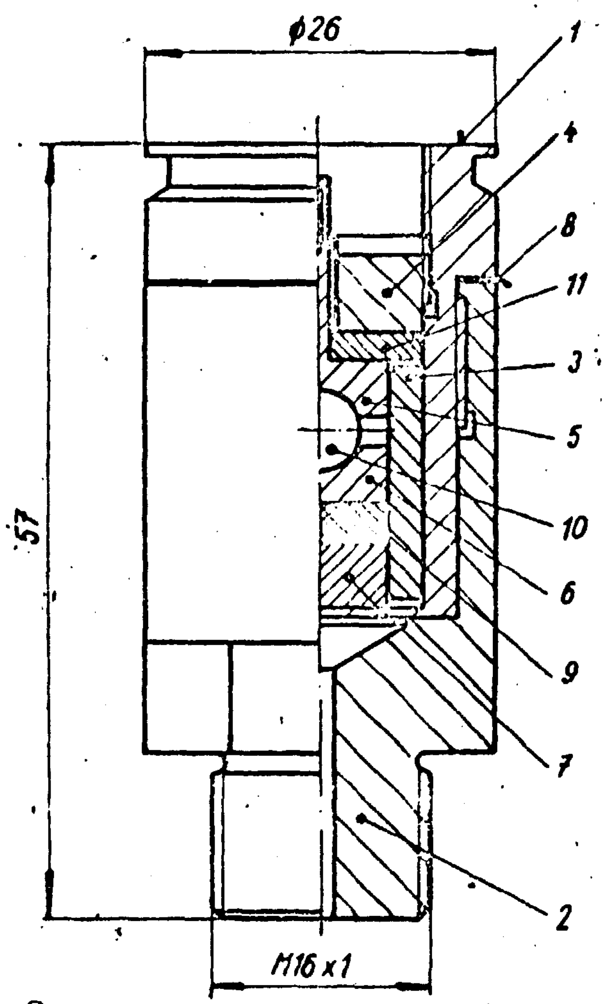

Fig. 8.

1 - body of the sensor 2 - bushing 3 - insulation
4 - nut 5 - collecting electrode 6 - support
7 - converting member 8 - sealing 9 - crystal
10 - ball 11 - insulation

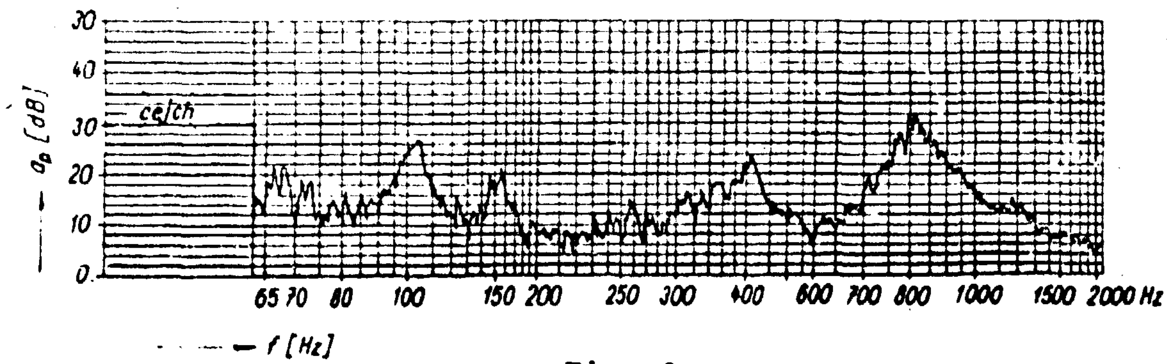

Fig. 9.

10 dB = 0,005 MPa

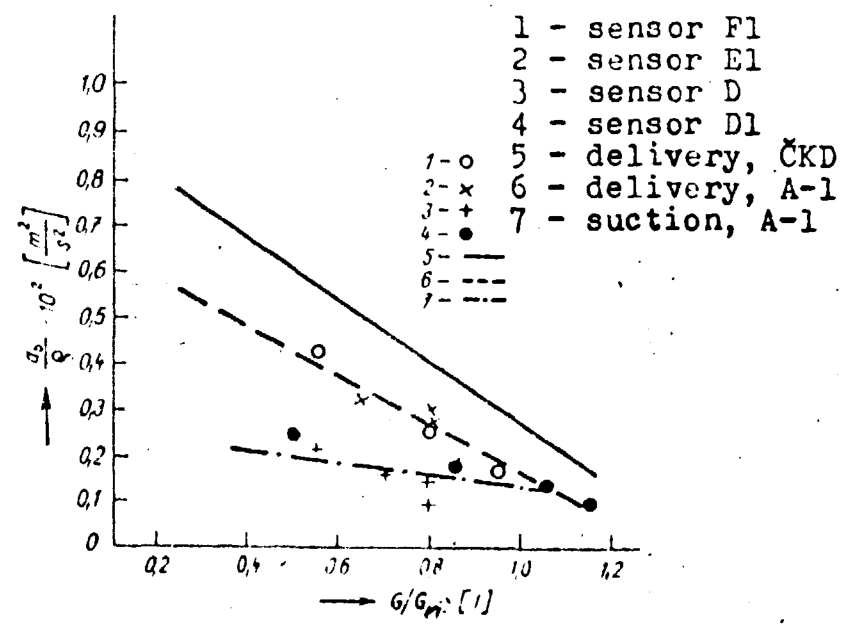

Fig. 10.

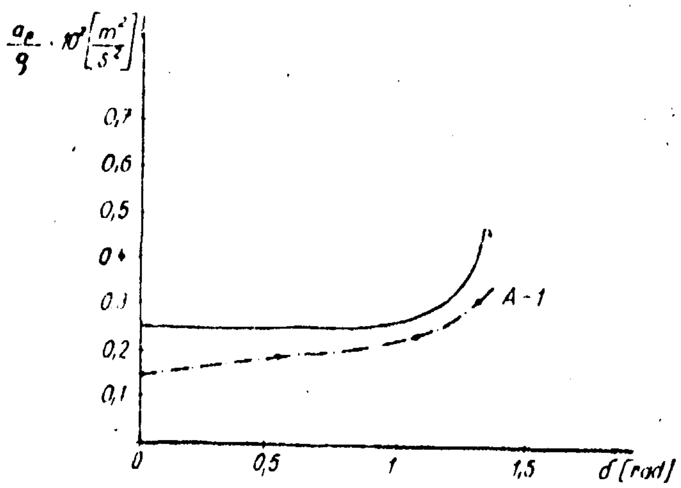

Fig. 11.

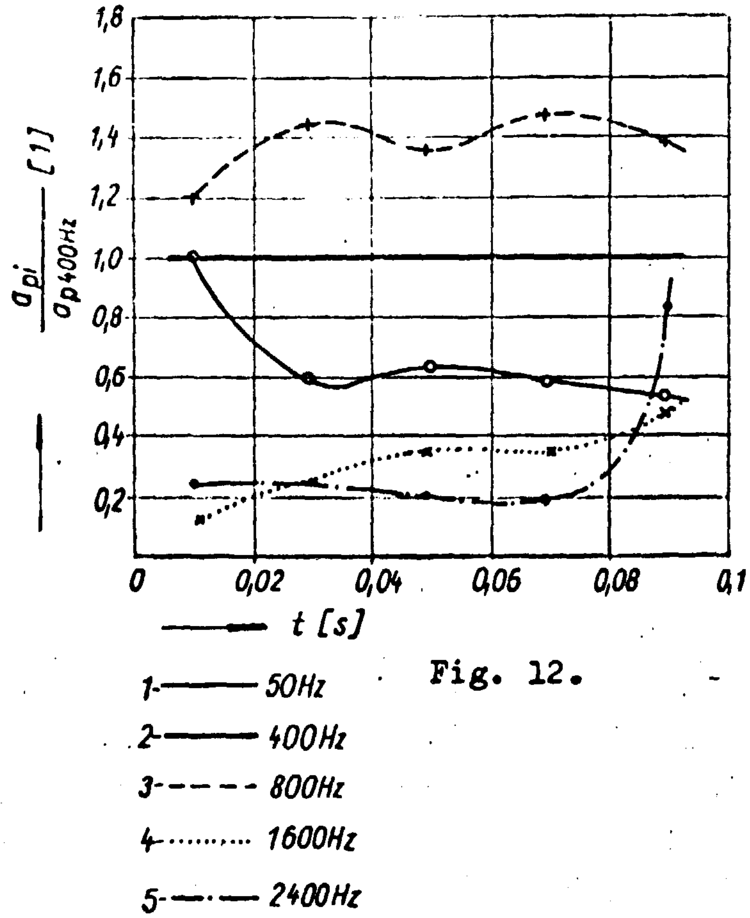
1,8
1,6
1,4
1,2
1,0
0,8
0,6
0,4
0,2
0
0,02
0,04
0,06
0,08
0,1
$\frac{a_{pi}}{a_{p400Hz}}$ [1]
t [s]
1- 50Hz
2- 400Hz
3- 800Hz
4- 1600Hz
5- 2400Hz

Fig. 12.

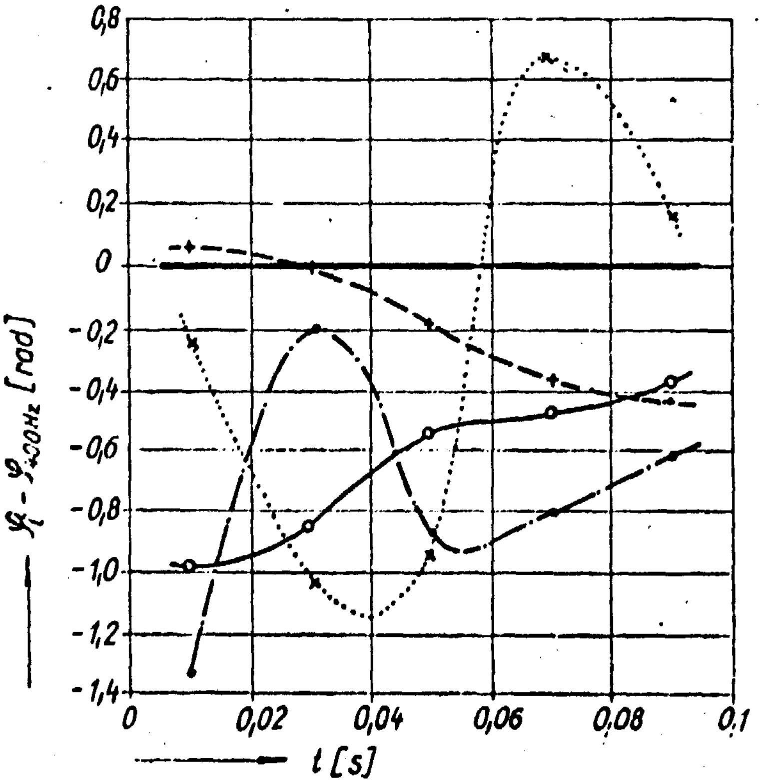
0,8
0,6
0,4
0,2
0
-0,2
-0,4
-0,6
-0,8
-1,0
-1,2
-1,4
0
0,02
0,04
0,06
0,08
0,1
$\varphi_i - \varphi_{400Hz}$ [rad]
t [s]

Fig. 13.